[5] Messiter, A. F., "A similarity law for the normal force on a delta wing at hypersonic speeds," J. Aero/Space Sci. 26, 119–120 (1959).

[6] Cole, J. D., "Sweepback theory for shock waves at hypersonic speeds," Rand Rept. RM-1991 (1957).

[7] Hida, K., "Blunt body theory for hypersonic flow," Air Force Office Sci. Research 204, Calif. Inst. Tech. (1961).

[8] Smith, F. M., "Experimental and theoretical aerodynamic characteristics of two low-aspect-ratio delta wings at angles of attack to 50° at a Mach number of 4.07," NACA RM L57E02 (1957); declassified.

[9] Bertram, M. H. and McCauley, W. D., "An investigation of the aerodynamic characteristics of thin delta wings with a symmetrical double-wedge section at a Mach number of 6.9," NACA RM L55B14 (1955); declassified.

[10] Kaattari, G. E., "Pressure distributions on triangular and rectangular wings to high angles of attack—Mach numbers 2.46 and 3.36," NACA RM A54J12 (1955); declassified.

[11] Hill, W. A., Jr., "Experimental lift of low-aspect-ratio triangular wings at large angles of attack and supersonic speeds," NACA RM A57117 (1957); declassified.

[12] Nicholson, K. F., "The effects of blunt leading edges on delta wings at M = 5.8," A. E. Thesis, Calif. Inst. Tech. (1958).

[13] Kennet, H., "The inviscid hypersonic flow on the windward side of a delta wing," Inst. Aerospace Sci. Paper 63-55 (January 1963).

APRIL 1963 AIAA JOURNAL VOL. 1, NO. 4

Performance Evaluation of a Magnetically Spun d.c. Arc Operating in Nitrogen

D. R. BOLDMAN*

NASA Lewis Research Center, Cleveland, Ohio

The results of an experimental investigation of a concentric cylinder-type electrode configuration incorporating a magnetic field indicated that the arc potential difference in nitrogen was essentially independent of the pressure in the range of 1 to 7 atm except for a specific range of operating conditions in which a 26% increase in arc potential difference was obtained. Highest efficiencies were achieved during the high potential operating mode. The independent effect of the electromagnetic force on the arc is not conclusive; however, experiments in which the magnetic field strength was varied over a moderate range indicated the importance of optimizing this effect from the standpoint of both chamber efficiency and arc stability. Photographs of the arc reveal some of the effects of varying the magnetic field strength. The arc chamber efficiency was influenced also by the flow injection mode. An increase in efficiency was obtained when the flow opposed or was normal to the direction of the Lorentz force.

Introduction

AEROSPACE applications of the electric arc have introduced a number of new problem areas associated with the development of efficient, high-power arc chambers. One method, currently employed, to improve the performance of the high-power arc chamber consists of using electromagnetic forces to spin the arc at very high angular speeds. Such forces can be either self-induced[1] or applied by independent means as in Ref. 2 and the work to be described herein.

Electrode Design and Limitations

Thoriated-Tungsten Cathode

There are several advantages peculiar to this type of cathode. The arc becomes attached firmly to the pointed tip, as shown in Fig. 1, so that one end is fixed in space, thus providing good control of the longitudinal position of the arc. Clean operation (contamination rates less than 0.1% by weight) for periods of several hours is possible if the cathode current limit is not exceeded.

A pointed tip has an advantage over the blunt tip from the standpoint of ease in starting; however, a blunt tip can conduct a higher current. The current limit of a 0.75-in.-diam pointed thoriated-tungsten cathode is approximately 1000 amp in nitrogen at pressures of 0.5 to 5 atm. The current limit for a 0.75-in.-diam flat-tipped cathode is about 1200 amp under the same conditions; however, increasing the diameter of the flat tip to 1 in. permits operation at about 1500 amp with little contamination. A 0.75-in.-diam pointed tip can be employed in argon environments at current levels exceeding 5000 amp. Since the cathodes are current-limited, higher power levels can be achieved by either using multiple cathodes[3, 4] or combining several units with a common plenum.[5]

Water-Cooled Copper Anode

The anode consists of a water-cooled (coolant flow velocity of 16 fps at 60 psi gage) copper cylinder wound with a field coil (Fig. 1). Maximum magnetic flux densities of about 2.0 kgauss have been used. The anode has been subjected to several hours of operation at currents as high as 2100 amp (using multiple cathodes) in nitrogen at a pressure of 2 atm. In argon the anode has operated for several minutes at a current of 5200 amp and a pressure of 0.5 atm. The maximum power input in both nitrogen and argon environments is about 500 kw for the forementioned coolant flow and magnetic flux density.

Performance

Evaluation Procedure

In the performance evaluation, four variables were controlled independently, namely: 1) the arc power input,

Presented at the ARS Electric Propulsion Conference, Berkeley, Calif., March 14–16, 1962; revision received January 11, 1963.

* Aerospace Research Engineer. Member AIAA.

2) the nitrogen mass-flow rate, 3) the nozzle throat diameter, and 4) the magnetic flux density. The data were cross-plotted so that the absolute variation of the important arc characteristics with the basic parameters could be determined.

Since for a given mass-flow rate the stagnation pressure is primarily a function of the nozzle throat diameter, the effect of stagnation pressure on arc heater performance was obtained by using nozzles with different throat diameters. A performance evaluation was conducted for the configuration of Fig. 2 using a single 0.75-in.-diam blunt-tipped thoriated-tungsten cathode with a 2.5-in.-diam by 7-in.-long anode in conjunction with various sizes of converging-diverging nozzles. This configuration was selected because the simplicity of the design expedited disassembly for frequent inspection of the electrodes and also because the electrode geometry remained fixed (low contamination rates) for running times of several hours (provided the current limit of the cathode was not exceeded). In this phase of the investigation, the gas was injected in a vortex in the direction of the Lorentz force. The magnetic flux density distribution was held constant—a maximum value of 2.0 kgauss at the center of the anode.

Arc Potential Characteristics

The arc potential decreased with increasing current and increased with increasing nitrogen flow. A rather strange effect of pressure on potential is shown in Fig. 3 for an arc current of 1000 amp. If the curves for all except the 0.25-in.-throat-diam nozzle are considered, the arc potential would be apparently insensitive to the pressure in the range of 1 to 7 atm. However, the 0.25-in.-throat-diam nozzle data indicate a change in the arc mode.

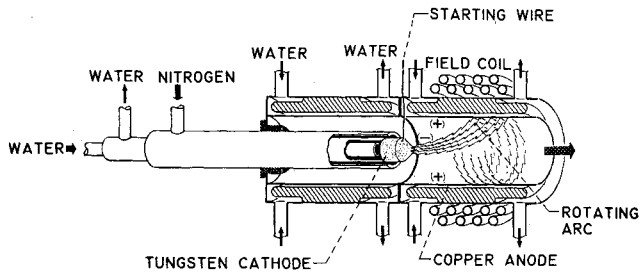

Fig. 1 Magnetically spun d.c. arc (original version, Ref. 2)

A higher arc potential difference can be noted on either side of the transition region, indicating that the 0.25-in.-diam nozzle might be the optimum size for the range of conditions investigated. It will be shown later that the high potential operating mode results in a better arc chamber efficiency.

The transition to a higher arc potential was observed to be a region of unstable arc behavior; therefore, a smooth curve between these flow rates could not be constructed. A similar transition in the arc potential characteristic was noted also in the modified version of this arc chamber.[3, 4] Unfortunately, such phenomena cannot be explained at this time; however, experiments have shown that the unstable operation in the transition region can be controlled to some extent by increasing the magnetic flux density.

Component Losses and Chamber Efficiency

The losses of the cathode and cathode chamber (water-cooled section that separates the anode and cathode), anode, and nozzle are considered separately. The cathode loss to the cooling water is small (generally about 5% of the total arc power) for the thoriated tungsten. There is also an additional radiation loss from the incandescent tip which has been calculated to be less than 1.0% of the power input.

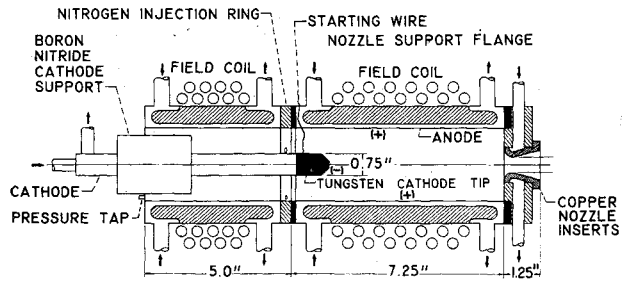

Fig. 2 Arc chamber for study of effects of pressure on operating parameters

The cathode chamber is exposed to radiation from the arc, and this heat loss is of the same order of magnitude as that of the cathode.

The anode heat loss includes the usual product of the anode sheath potential difference and the current, in addition to the forced-convection loss of the heated gas. There is also radiation from the arc filaments to the cold wall which is believed to be relatively small for the pressure levels considered here.[6] The component losses divided by the arc power for three of the five nozzles are shown in Figs. 4a–4c. The combined cathode and cathode chamber losses (indicated as cathode loss in the figures) ranged from about 1 to 8% of the total power input, decreasing slightly with increasing flow rate. Nozzle losses were generally less than 5% of the power input for the entire range of operating conditions. The heat transfer rate to the anode represents by far the greatest loss in the system. Anode losses ranged from 30 to 83% of the power input, depending upon the pressure and operating mode. The greatest anode losses occurred during high-pressure operation with the 0.125-in. nozzle.

The arc chamber efficiency is defined as the percentage of the arc power invested as useful energy in the gas prior to the nozzle expansion process. Efficiency computations are based on the heat loss to the electrodes and supporting chamber and do not include losses to the nozzle, ballast resistor, field coil, or power supply. The high potential operating mode is the more efficient mode, as shown by the curves for the 0.25-in.-throat-diam nozzle (Fig. 5).

Since better efficiencies were obtained during periods of high arc potential operation, attempts were made to stretch the arc by withdrawing the cathode into the back chamber; however, the arc moved upstream with the cathode, which caused secondary arcing across these components. In fact, this tendency to arc to the rear chamber was so strong that a 0.25-in.-thick coating of alumina failed to eliminate the secondary arc. This type of operation occurred with both nitrogen and argon.

Attempts to establish the anode convection heat transfer effects arising from a reduction in "wetted" area were unsuccessful because the arc characteristic changed appreciably when the cathode was moved to a downstream position (ap-

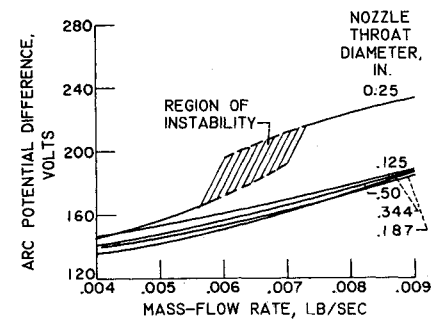

Fig. 3 Effect of pressure on arc potential difference (arc current = 1000 amp)

proximately in the center of the anode). The lower arc potential drop in this region was attributed to a reduction in the gas-arc interaction volume (see Fig. 2). Arc heater efficiencies were actually lower for the same input power with the cathode in the downstream position.

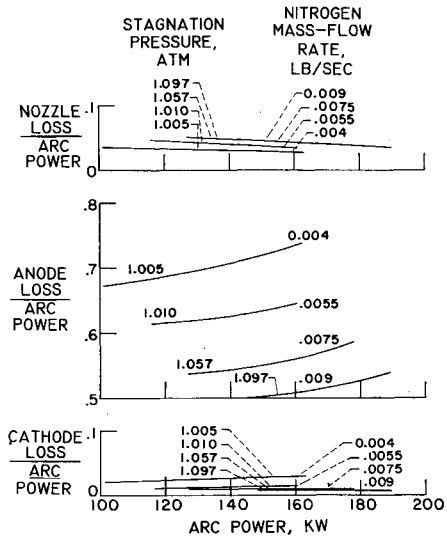

Fig. 4a Component heat losses; nozzle throat diameter, 0.50 in.

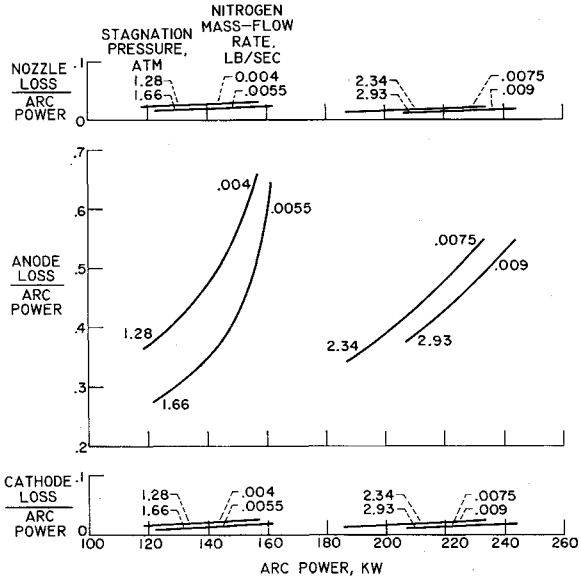

Fig. 4b Component heat losses; nozzle throat diameter, 0.25 in.

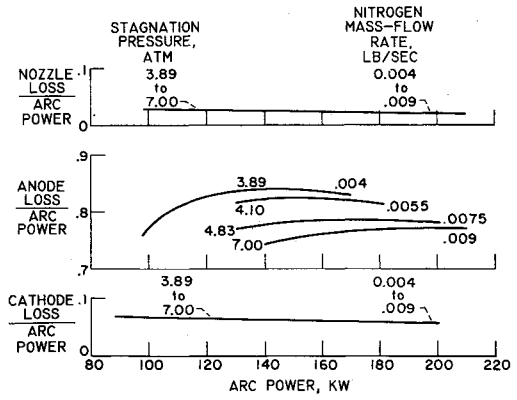

Fig. 4c Component heat losses; nozzle throat diameter, 0.125 in.

Magnetic Field Effects

The arc was photographed after removing the nozzle supporting flange. High-speed motion pictures reveal the diffuse nature of the arc indicated in Ref. 3. The arc appeared to be so diffuse that rotational speeds with a maximum flux density of only 1.2 kgauss could not be determined at film speeds of 4000 frames/sec. The exposure time for these photographs was approximately 4 μsec. Three types of operating conditions have been photographed at a constant mass-flow rate and are shown in Figs. 6a–6c. The diffuse arc is shown in Fig. 6a. In Fig. 6b, the magnetic flux density was reduced by a factor of 2, and the arc appeared to attain a fixed position favoring a spot near the periphery of the cathode. Consequently, the arc potential was reduced considerably. The vortex flow direction was reversed in Fig. 6c; however, the erratic nature of the arc is still apparent. At the same input power and flow rate, the efficiency increased slightly over the value corresponding to the operating condition portrayed in Fig. 6b. This might be expected, because the gas and arc exposure time is increased.

The variation of the arc chamber efficiency with magnetic field strength at higher input powers and mass-flow rates is shown in Fig. 7. It should be emphasized that, although the field strength in some cases is lower than that of Figs. 6b and 6c, the diffuse arc characteristic was maintained for all the data presented in Fig. 7 because of the higher arc current and mass-flow rate. Several regions of unstable operation occurring between plateaus of stable performance can be noted. Also, a strange hysteresis-type behavior occurred at both flow rates (elapsed time of complete test at constant mass-flow rate and power was about 30 min). This effect, which is most pronounced for the high-power condition, occurred as the result of a change in arc potential difference between the start and conclusion of the test. The sequence of operation shown in Fig. 7 is not required in order to arrive at the end-point operating conditions. A slight adjustment of the magnetic flux density in the neighborhood of 1.7 kgauss resulted in a more efficient mode, thus indicating the possibility of an unstable starting point. At the low flow condition, there appears to be an optimum operating range in the neighborhood of 0.7 kgauss; however, the efficiency was relatively insensitive to the field strength at the high flow condition. At fields below approximately 0.4 kgauss the arc becomes too unstable for practical applications.

Flow Injection Effects

The efficiency of the arc chamber is influenced by the flow injection mode as shown in Fig. 8. Axial flow injection and flow opposing the Lorentz force tend to create a higher arc potential difference than flow in the direction of the Lorentz force, thus resulting in a higher efficiency.

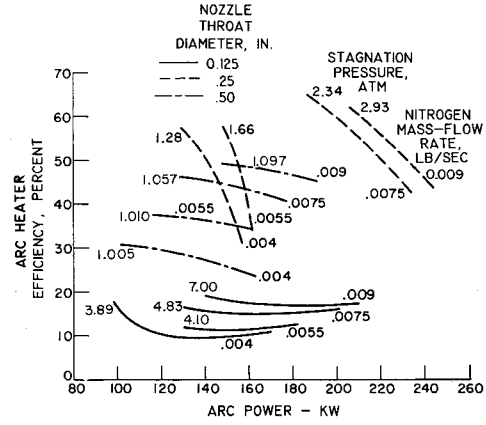

Fig. 5 Archeater efficiency

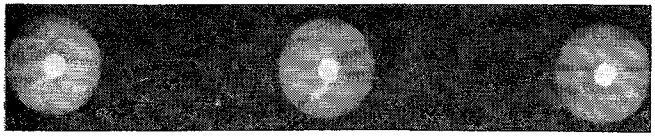

a) Field strength = 1.2 kgauss; emf and flow in counterclockwise direction

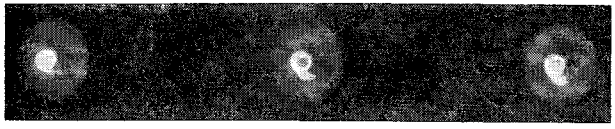

b) Field strength = 0.6 kgauss; emf and flow in counterclockwise direction

c) Field strength = 0.6 kgauss, emf clockwise and flow counterclockwise

Fig. 6 Magnetically spun arc (4000 frames/sec); nitrogen flow rate, 0.006 lb/sec

Preliminary tests in which the electrode configuration was modified by inserting a nozzle-type flow constrictor over the cathode tip have been very encouraging. The constrictor provides a high-velocity jet over the tungsten tip and increases the arc potential difference and efficiency.

Concluding Remarks

The Lorentz forces used to spin the arc were beneficial from the standpoint of reduced anode erosion rates, more uniform mixing, and greater arc stability. The degree to which these factors were influenced favorably became greater with stronger magnetic fields.

Efficiency gains generally were obtained by increasing the arc potential difference at constant power and flow rate. Abrupt changes in the arc potential difference (resistance) were observed, especially at low values of magnetic flux density; however, such changes were difficult to predict and control. The arc potential difference could be controlled to some extent by altering the flow injection scheme. An increase in potential difference occurred when the flow was injected normal to or opposite the direction of the Lorentz force, thus resulting in a higher efficiency. Preliminary tests have indicated that further improvements in the arc potential difference and efficiency are attainable by using a flow constrictor to produce a high-velocity gas jet over the cathode tip.

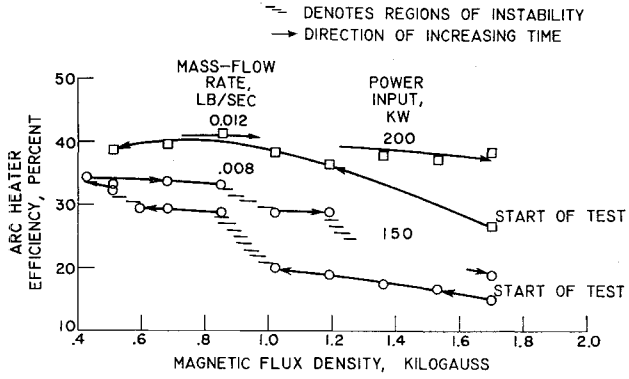

Fig. 7 Effect of magnetic field on efficiency

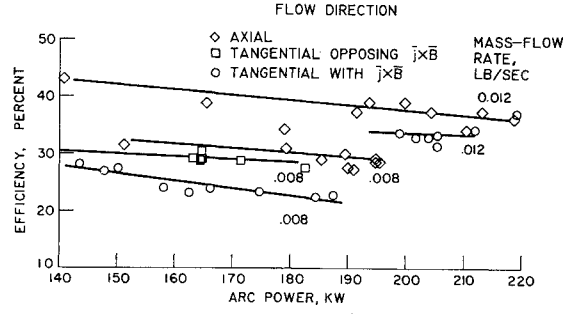

Fig. 8 Effect of flow injection scheme on efficiency

References

[1] Reid, J. W., "Recent advances to high pressure, high power arcs," ARS Preprint 2127-61 (October 1961).

[2] Shepard, C. E. and Boldman, D. R., "Preliminary development of electrodes for an electric-arc wind tunnel," NASA Memo. 4-14-59E (1958).

[3] Shepard, C. E. and Winovich, W., "Electric-arc jets for producing gas streams with negligible contamination," Am. Soc. Mech. Engrs. Annual Winter Meeting Preprint 61-WA-247 (November 1961).

[4] Boldman, D. R., Shepard, C. E., and Fakan, J. C., "Electrode configurations for a wind-tunnel heater incorporating the magnetically spun electric arc," NASA TN D-1222 (1962).

[5] Rose, P. H., Powers, W. E., and Hritzay, D., "A large high pressure arc plasma generator: a facility for simulating missile and satellite re-entry," Avco Research Rept. 56 (June 1959).

[6] Stadler, J. R., Goodwin, F. K., Ragent, B., and Noble, C. E., "Aerodynamic applications of plasma wind tunnels," Vidya Inc., Palo Alto, Calif., Rept. 18 (February 1960).